International Journal of Engineering & Applied Sciences (IJEAS)
Vol.9, Issue 2 (Special Issue: Composite Structures) (2017) 112-126
http://dx.doi.org/10.24107/ijeas.318459
Int J Eng Appl Sci 9(2) (2017) 112-126

Exact Thermal Analysis of Functionally Graded Cylindrical and Spherical Vessels

Vebil Yıldırım

University of Çukurova, Department of Mechanical Engineering
E-mail address: vebil@cu.edu.tr

Received date: June 2017
Accepted Date: July 2017

Abstract

Thermal analyses of radially functionally graded (FG) thick-walled a spherical vessel and an infinite cylindrical vessel or a circular annulus are conducted analytically by the steady-state 1-D Fourier heat conduction theory under Dirichlet's boundary conditions. By employing simple-power material grading pattern the differential equations are obtained in the form of Euler-Cauchy types. Analytical solution of the differential equations gives the temperature field and the heat flux distribution in the radial direction in a closed form. Three different physical metal-ceramic pairs first considered to study the effect of the aspect ratio, which is defined as the inner radius to the outer radius of the structure, on the temperature and heat flux variation along the radial coordinate. Then a parametric study is performed with hypothetic inhomogeneity indexes for varying aspect ratios.

Keywords: Thermal analysis; functionally graded; exact solution; axisymmetric; cylindrical vessel, spherical vessel, inhomogeneity index, aspect ratio, thick-walled, circular annulus.

1. Introduction

As is well known, a temperature difference results in the heat conduction and the heat transfer in structures. Manufacturing processes in factories generally include thermal processes. So the thermal analysis is an important issue in industry related to mechanical, chemical, automotive, petroleum, nuclear engineering and living tissues. A thermal analysis is also the back-bone for the thermal-related analyses such as thermo-mechanical, thermo-electro-mechanical etc. So an accurate solution to the temperature field in the structure is always be very helpful for understanding the real physical thermal response of the structure under consideration at both the manufacturing phase and during its life-time.

To explore the question a number of studies were performed analytically, numerically and experimentally up to now. Chang and Tsou [1-2] used the Green's functions for heat conduction in an anisotropic medium for both steady state and unsteady state cases. Oato et al. [3] studied axisymmetric, transient, thermal stress analysis of a hollow cylinder composed of multilayered composite laminates with temperature changes in the radial and axial directions due to axisymmetric heating from the outer and/or the inner surfaces. They used Fourier cosine transform and Laplace transform for the temperature field and the thermo-elastic potential function and apply Love's displacement function to the thermo-elastic field. They then obtained the exact solutions for the temperature and thermal stress distributions in a transient state. Obata and Noda [4] studied the steady thermal stresses in a hollow cylinder and a hollow sphere made of a functionally gradient material (FGM) and compared their results with those of a FGM plate. Zimmerman and Lutz [5] derived an exact solution for the problem of the uniform heating of FG circular cylinder whose modulus of elasticity and thermal expansion coefficient vary linearly with radius. Tarn [6] found an exact solution for FG anisotropic cylinders subjected to thermal and mechanical loads. Awaji and Sivakumar [7] presented a numerical technique for analyzing one dimensional transient temperature distributions in a circular hollow cylinder that was composed of functionally graded ceramic–metal-based materials, with considering the temperature-dependent material properties. A 1-D steady state mechanical and thermal stress analysis of a thick hollow cylinder under axisymmetric and non-axisymmetric loads was studied by Jabbari et al. [8-10]. Liew et al. [11] sectioned the FGM cylinder into a number of homogeneous sub-cylinders. Displacements and stresses within the homogeneous sub-cylinders are obtained from the homogeneous solutions in Reference [11]. Tarn and Wang [12] worked the end effects of heat conduction in circular cylinders of functionally graded materials and laminated composites. Ruhi et al. [13] presented a semi analytical thermo-elasticity solution for thick-walled finite-length cylinders made of power-graded materials. The stress distribution in a power-graded orthotropic cylindrical body was investigated analytically by Oral and Anlaş [14]. Eslami et al [15] offered a general solution for the one-dimensional steady-state thermal and mechanical stresses in a hollow thick sphere made of a simple-power graded material. By using the Laplace transformation and a series expansion of Bessel functions, Ootao and Tanigawa [16] analyzed one-dimensional transient thermoelastic problem with power-law graded material properties. Pelletier and Vel [17], by using an arbitrary variation of orthotropic material properties in the radial direction, studied analytically the steady-state response of a functionally graded thick cylindrical shell subjected to thermal and mechanical loads and simply supported at the edges by the power series method. Birman and Byrad [18] reviewed related studies published in 2000-2007.

After 2007s, one-dimensional studies are focused especially on the transient thermal analysis, the stress and deformation analyses under steady state case etc. Kayhani et al. [19] presented an exact solution of conductive heat transfer in a cylindrical composite laminate in the radial and azimuthal directions. Kayhani et al. [20] further obtained a general analytical solution for heat conduction in cylindrical multilayered composite laminates in the radial and axial directions. Hosseini and Abolbashari [21] presented a unified formulation to analyze of temperature field in a thick hollow cylinder made of functionally graded materials with various grading patterns. Bayat et al. [22] carried out a thermo-mechanical analysis of functionally graded hollow sphere subjected to mechanical loads and one-dimensional steady-state thermal stresses. Lee and Huang [23] developed an analytic solution method, without integral transformation, to find the exact solutions for the transient heat conduction in functionally graded (FG) circular hollow cylinders with time-dependent boundary conditions. By introducing suitable shifting functions, the governing second-order regular singular differential equation with variable coefficients and time-dependent boundary conditions is transformed into a differential equation with homogenous boundary conditions. In Lee and Huang’s [23] study, while the density has a constant value, the variation of specific heat is considered. Wang [24] developed an effective approach to analyze the transient thermal analysis in a functionally graded hollow cylinder based on the laminate approximation theory. The heat conductivity, mass density and specific heat are assumed to vary along the radial direction with arbitrary grading pattern as in the study. Wang [24] divided the transient solution into two parts. He obtained the quasi-static solution by the state space method and the dynamic solution by the initial parameter method in the time domain. By dividing the cylinder into some homogeneous sub-cylinders, an arbitrarily-graded circular hollow cylinder is studied analytically under arbitrarily non-uniform loads on the inner and outer surfaces by Li and Liu [25]. Delouei and Norouzi [26] presented an exact analytical solution for unsteady conductive heat transfer in multilayer spherical fiber-reinforced composite laminates for the most generalized linear boundary conditions consisting of the conduction, convection, and radiation. Arefi [27] performed a nonlinear thermal analysis of a hollow functionally graded cylinder by employing a semi-analytical method of successive approximations. A power function distribution is used for the simulation of non-homogeneity of the material used. A temperature dependence is employed for only the thermal conductivity. Based on the two-points Hermite approximations for integrals, Chen and Jian [28] proposed an improved lumped parameter model for the transient thermal analysis of multilayered composite pipeline with active heating. Daneshjou et .al. [29] presented a non-Fourier heat conduction analysis of infinite 2-D functionally graded (FG) hollow cylinders subjected to a time-dependent heat source. In Daneshjou et .al.'s study [29], a new augmented state space method considering laminate approximation theory is introduced. All material properties are assumed to vary continuously within the cylinder along the specified directions following an arbitrary law.

As seen from the literature survey that the thermal-related analyses are of great importance for both cylindrical and spherical structures. However, most of those studies focused on the computation of thermal stresses in the structure. That is, although they implemented the temperature distribution in their analyses, the thermal behavior of such structures were not studied in a detailed manner. In the present study, because of these reasons, the thermal analysis of such structures is addressed individually for both spherical and cylindrical vessels made of functionally power-law-graded non-homogeneous materials. It may be noted that the heat conduction equations are identical for both a cylindrical structure and a uniform discs or a circular annulus.

2. Derivation and Solution of Heat Conduction Equations

The rate of the heat flux in a solid object is directly proportional to the temperature gradient. The Fourier law governing the heat transfer by conduction is

$$\boldsymbol{q} = -k\nabla T = -k \ grad \ (T) \tag{1}$$

where the temperature gradient is given in cylindrical coordinates, $T(r,\theta,z,t)$, by

$$\nabla T = \frac{\partial T}{\partial r}\boldsymbol{e}_r + \frac{1}{r}\frac{\partial T}{\partial \theta}\boldsymbol{e}_\theta + \frac{\partial T}{\partial z}\boldsymbol{e}_z \tag{2a}$$

and in spherical coordinates, $T(r,\theta,\varphi,t)$, by

$$\nabla T = \frac{\partial T}{\partial r}\boldsymbol{e}_r + \frac{1}{r}\frac{\partial T}{\partial \theta}\boldsymbol{e}_\theta + \frac{1}{r\sin\theta}\frac{\partial T}{\partial \varphi}\boldsymbol{e}_\varphi \tag{2b}$$

By using the first law of thermodynamics, the heat conduction equation is written as follows

$$\rho c_p \frac{\partial T}{\partial t} + div(\boldsymbol{q}) = \dot{q}_{gen} \tag{3}$$

This equation takes the following form without heat generation in the structure [30].

$$\nabla^2 T = \frac{\rho c_p}{k}\left(\frac{\partial T}{\partial t}\right) = \kappa \frac{\partial T}{\partial t} \tag{4}$$

Where Laplacian of the temperature is derived in cylindrical coordinates as

$$\nabla^2 T = \Delta T = \nabla \bullet \nabla T = \frac{1}{r}\frac{\partial}{\partial r}(r\frac{\partial T}{\partial r}) + \frac{1}{r^2}\frac{\partial^2 T}{\partial \theta^2} + \frac{\partial^2 T}{\partial z^2} \tag{5a}$$

and in spherical coordinates as follows

$$\nabla^2 T = \Delta T = \nabla \bullet \nabla T = \frac{1}{r^2}\frac{\partial}{\partial r}(r^2\frac{\partial T}{\partial r}) + \frac{1}{r^2 \sin\theta}\frac{\partial}{\partial \theta}(\sin\theta \frac{\partial T}{\partial \theta}) + \frac{1}{r^2 \sin^2\theta}\frac{\partial^2 T}{\partial \varphi^2} \quad (5b)$$

In recent years functionally graded metal-ceramic composites gain considerable attention due to their attractive properties such as heat resisting, erosion and corrosion resistant, and fracture toughness. For the one-dimensional axisymmetric conditions, $\frac{\partial}{\partial \theta} = 0, \frac{\partial}{\partial \varphi} = 0, \frac{\partial}{\partial z} = 0$, the non-steady heat conduction equation of such materials in which the thermal conductivity, density, and the specific heat change along the radial direction becomes (Fig. 1)

$$\frac{1}{r^2}\frac{\partial}{\partial r}\left(r^2 k(r,t)\frac{\partial T(r,t)}{\partial r}\right) = \rho(r,t)c_p(r,t)\frac{\partial T(r,t)}{\partial t} \quad \text{(sphere)} \quad (6a)$$

$$\frac{1}{r}\frac{\partial}{\partial r}\left(r k(r,t)\frac{\partial T(r,t)}{\partial r}\right) = \rho(r,t)c_p(r,t)\frac{\partial T(r,t)}{\partial t} \quad \text{(cylinder/circular annulus)} \quad (6b)$$

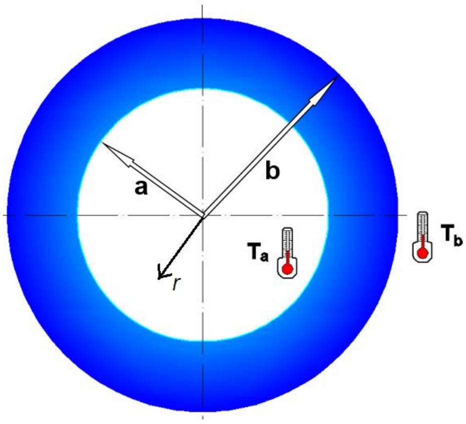

Fig.1. A characteristic section of the structure

After re-arranging of the equations given above, one may get the followings for the spherical structure

$$\frac{\partial^2 T(r,t)}{\partial r^2} + \frac{\partial T(r,t)}{\partial r}\left(\frac{2}{r} + \frac{\frac{\partial k(r,t)}{\partial r}}{k(r,t)}\right) = \frac{\rho(r,t)c_p(r,t)}{k(r,t)}\frac{\partial T(r,t)}{\partial t} \quad (7a)$$

for the cylindrical structure or a disk of uniform thickness or a circular annulus

$$\frac{\partial^2 T(r,t)}{\partial r^2} + \frac{\partial T(r,t)}{\partial r}\left(\frac{1}{r} + \frac{\frac{\partial k(r,t)}{\partial r}}{k(r,t)}\right) = \frac{\rho(r,t)c_p(r,t)}{k(r,t)}\frac{\partial T(r,t)}{\partial t} \quad (7b)$$

By using prime symbol for derivatives with respect to the radial coordinate, for the steady state case ($\frac{\partial T}{\partial t} = 0$) one may get the followings.

$$T''(r) + T'(r)\left(\frac{2}{r} + \frac{k'(r)}{k(r)}\right) = 0 \text{ (sphere)} \tag{8a}$$

$$T''(r) + T'(r)\left(\frac{1}{r} + \frac{k'(r)}{k(r)}\right) = 0 \text{ (cylinder/uniform disk)} \tag{8b}$$

In the above equations, the material grading pattern may be chosen arbitrarily. Solution method to be adopted strictly depends on the material grading pattern considered. Some limited grading rules such as a simple power material grading rule permit to get the differential equation with constant coefficients and offer an analytical solution. For arbitrary grading patterns, the differential equations with variable coefficients are confronted. Consequently in the thermal analysis with arbitrary material grading patterns, it is necessary to use an appropriate numerical technique in the solution process. The material gradation may also be done as full-ceramic at the inner surface and full-metal at the outer surface, or vise-verse, or metal-ceramic mixtures at both surfaces by considering the real working conditions of the structure. Finally, all types of boundary conditions such as Dirichlet's, Neumann's, Robin's and mixed boundary conditions may be applied to the solution of equations (8).

To get exact solutions, in the present study, it is assumed that the thermal conductivity is changed outwardly between the inner and outer surfaces as follows

$$k(r) = k_a \left(\frac{r}{a}\right)^{\gamma} \tag{9}$$

where the inhomogeneity index of a physical material may be determined by

$$\gamma = \frac{\ln\left(\frac{k_a}{k_b}\right)}{\ln\left(\frac{a}{b}\right)} \tag{10}$$

Equation (8) becomes homogeneous Euler-Cauchy type differential equation with constant coefficients under assumptions given in Eq. (9). The solution will be in the form of

$$T(r) = C_1 r^{\mu_1} + C_2 r^{\mu_2} \tag{11}$$

Equation (8) is solved with the first kind boundary conditions (Dirichlet)

$$T(a) = T_a \;\; ; \; T(b) = T_b \tag{12}$$

The solutions for each homogeneous/inhomogeneous material types are presented in Tables 1 and 2 for cylindrical and spherical vessels, respectively.

3. Examples with Physical Materials

Metal-ceramic pairs considered in the present study and their material properties are presented in Table 3. It is assumed that the inner surface is to be full-metal, and the outer surface is to be full-ceramic. Between the inner and the outer surfaces the material gradation obeys Eq. (9). The boundary conditions are determined as: $T_a = 220^o C$, and $T_b = 20^o C$. The geometrical properties of the structures are chosen as follows: $a = 0.5m$, $b = 1.0m$.

Table 1. Differential equations and their solutions for cylinders or uniform discs $\{k(r) = k_a (r/a)^\gamma\}$

Cylinder /Uniform Disc Made of a Homogeneous and Isotropic Material	
$\frac{T'(r)}{r} + T''(r)=0$	$T(r) = C_2 + C_1 lnr$ $C_1 = \frac{T_a - T_b}{lna - lnb}$ $C_2 = \frac{lnaT_b - T_a lnb}{lna - lnb}$ $T(r) = \frac{(-lnb + lnr)T_a + (lna - lnr)T_b}{lna - lnb}$ $= \frac{T_b lna - T_a lnb + (T_a - T_b)lnr}{lna - lnb}$ $q_r(r) = \frac{k_o(-T_a + T_b)}{r(lna - lnb)}$
Cylinder/Uniform Disc Made of a Power-Law-Graded Isotropic and Non-homogeneous Material	
$\frac{(1+\gamma)T'(r)}{r} + T''(r) = 0$	$T(r) = -\frac{r^{-\gamma}}{\gamma} C_1 + C_2$ $C_1 = \frac{\gamma a^\gamma b^\gamma (T_a - T_b)}{a^\gamma - b^\gamma}$ $C_2 = \frac{a^\gamma T_a - b^\gamma T_b}{a^\gamma - b^\gamma}$ $T(r) = \frac{r^{-\gamma}(-a^\gamma(b^\gamma - r^\gamma)T_a + b^\gamma(a^\gamma - r^\gamma)T_b)}{a^\gamma - b^\gamma}$ $= \frac{r^{-\gamma}(-b^\gamma r^\gamma T_b + a^\gamma(r^\gamma T_a + b^\gamma(-T_a + T_b)))}{a^\gamma - b^\gamma}$ $q_r(r) = -\frac{a^\gamma b^\gamma r^{-1-\gamma}(\frac{r}{a})^\gamma \gamma k_a (T_a - T_b)}{a^\gamma - b^\gamma}$

Table 2. Differential equations and their solutions for spherical vessels $\{k(r)=k_a(r/a)^{\gamma}\}$

Sphere Made of a Homogeneous and Isotropic Material

$$T''(r)+\frac{2}{r}T'(r)=0$$

$$T(r)=-\frac{C_1}{r}+C_2$$

$$C_1=\frac{ab(T_a-T_b)}{a-b}$$

$$C_2=\frac{aT_a-bT_b}{a-b}$$

$$T(r)=\frac{-brT_b+a(rT_a+b(T_b-T_a))}{(a-b)r}$$

$$q_r(r)=\left\{\frac{ab(T_b-T_a)k_o}{r^2(a-b)}\right\}$$

Sphere Made of a Power-Law-Graded Isotropic and Non-homogeneous Material

$$T''(r)+\left(\frac{2}{r}+\frac{\gamma}{r}\right)T'(r)=0$$

$$T(r)=\frac{r^{-1-\gamma}}{-1-\gamma}C_1+C_2$$

$$C_1=\frac{a^{\gamma+1}b^{\gamma+1}(T_a-T_b)(\gamma+1)}{a^{\gamma+1}-b^{\gamma+1}}$$

$$C_2=\frac{(T_a-T_b)a^{\gamma+1}}{a^{\gamma+1}-b^{\gamma+1}}+T_b$$

$$T(r)=\frac{r^{-1-\gamma}(-b^{1+\gamma}r^{1+\gamma}\mathrm{Tb}+a^{1+\gamma}(r^{1+\gamma}\mathrm{Ta}+b^{1+\gamma}(-\mathrm{Ta}+\mathrm{Tb})))}{a^{1+\gamma}-b^{1+\gamma}}$$

$$q_r(\mathrm{r})=\left\{-\frac{a^{1+\gamma}b^{1+\gamma}r^{-2-\gamma}(T_a-T_b)(1+\gamma)}{a^{1+\gamma}-b^{1+\gamma}}\right\}k(r)$$

$$=-\frac{a^{1+\gamma}b^{1+\gamma}r^{-2-\gamma}(\frac{r}{a})^{\gamma}(T_a-T_b)(1+\gamma)k_a}{a^{1+\gamma}-b^{1+\gamma}}$$

Table 3. Metal-ceramic pairs considered in the present study

	$k\ (\frac{W}{mK})$	Metal/Ceramic pair	γ
Nickel (Ni)	90.7	FGM-1	-6.22922
Silicon Nitride (Si_3N_4)	1.209	(Ni/Si_3N_4)	
Aluminum (Al)	204	FGM-2	-2.76073
Aluminum Oxide (Al_2O_3)	30.1	(Al/Al_2O_3)	
SUS-304 (Stainless Steel)	15.379	FGM-3	-3.11101
Zirconium Oxide (ZrO_2)	1.78	(SUS-304/ZrO_2)	

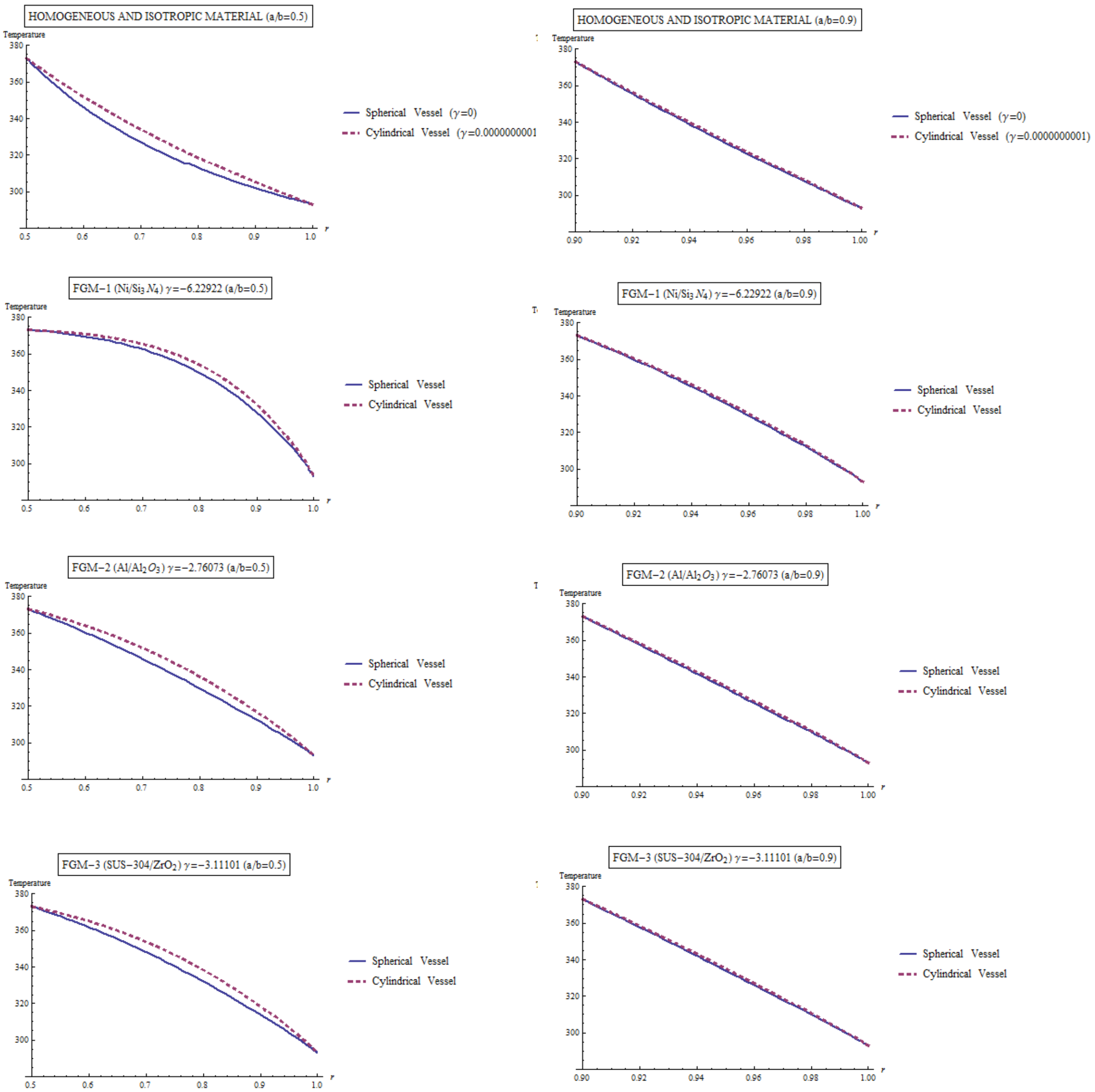

Fig. 2. Temperature variations in physical FGMs with the aspect ratio.

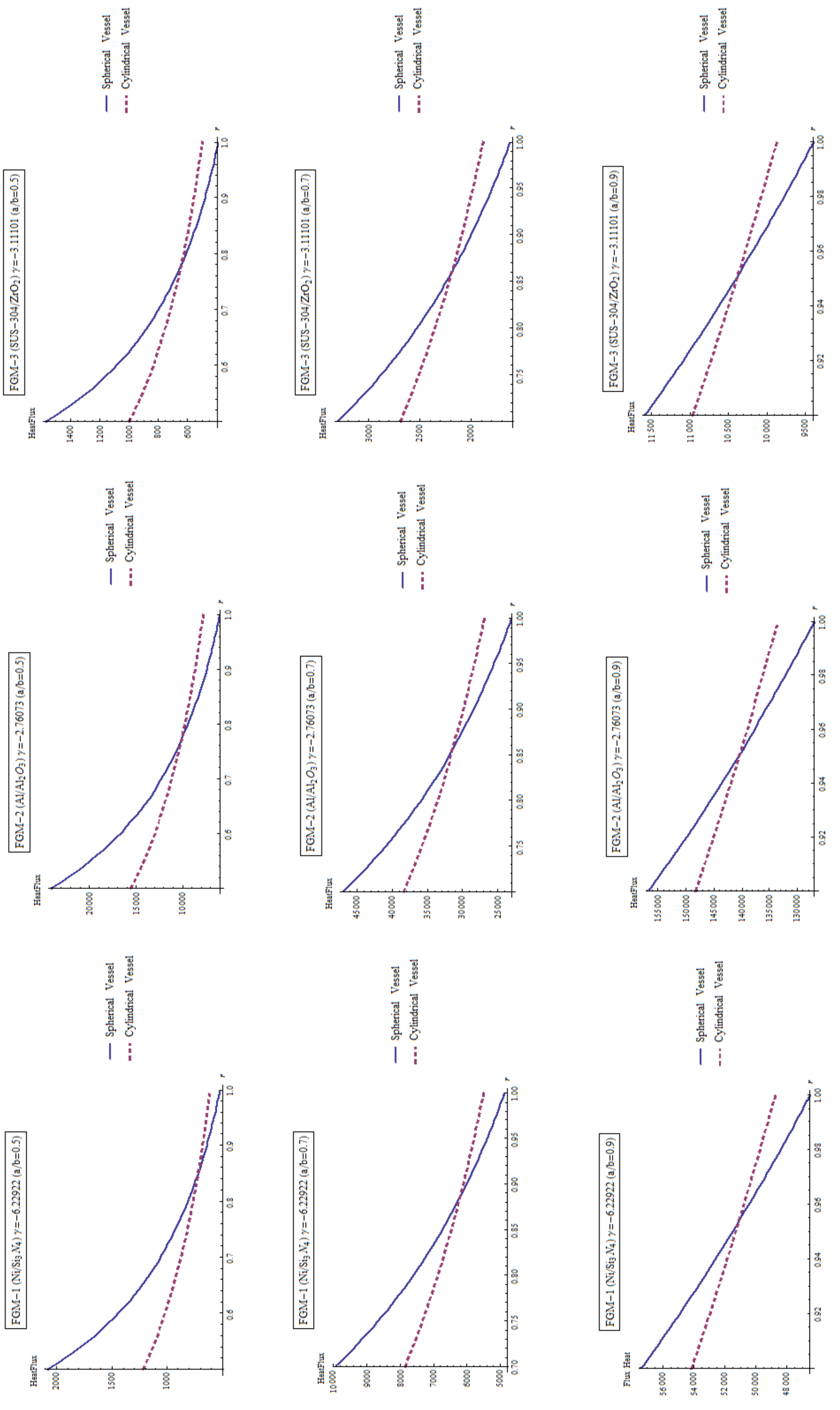

Fig. 3. Heat flux variations in physical FGMs with the aspect ratio.

Figs. 2 and 3 show the temperature and the heat flux variation in FGM-1, FGM-2 and FGM-3 metal-ceramic pairs for different aspect ratios. It is seen from Fig. 2 that the temperature change occurs somewhat rapid in spheres than cylinders. As the aspect ratio increases, that is when the thickness decreases, the temperature distribution differences between a cylinder and a sphere are facing disappearance. The temperature varies slowly in FGM-1 than the others. Heat flux in a sphere is higher than a cylinder as seen Fig. 3. An increase in the aspect ratio results much heat flux in the structure. The maximum heat flux occur at the inner surface of both structural geometries. FGM-2 offers the best metal-ceramic pair regarding the heat flux.

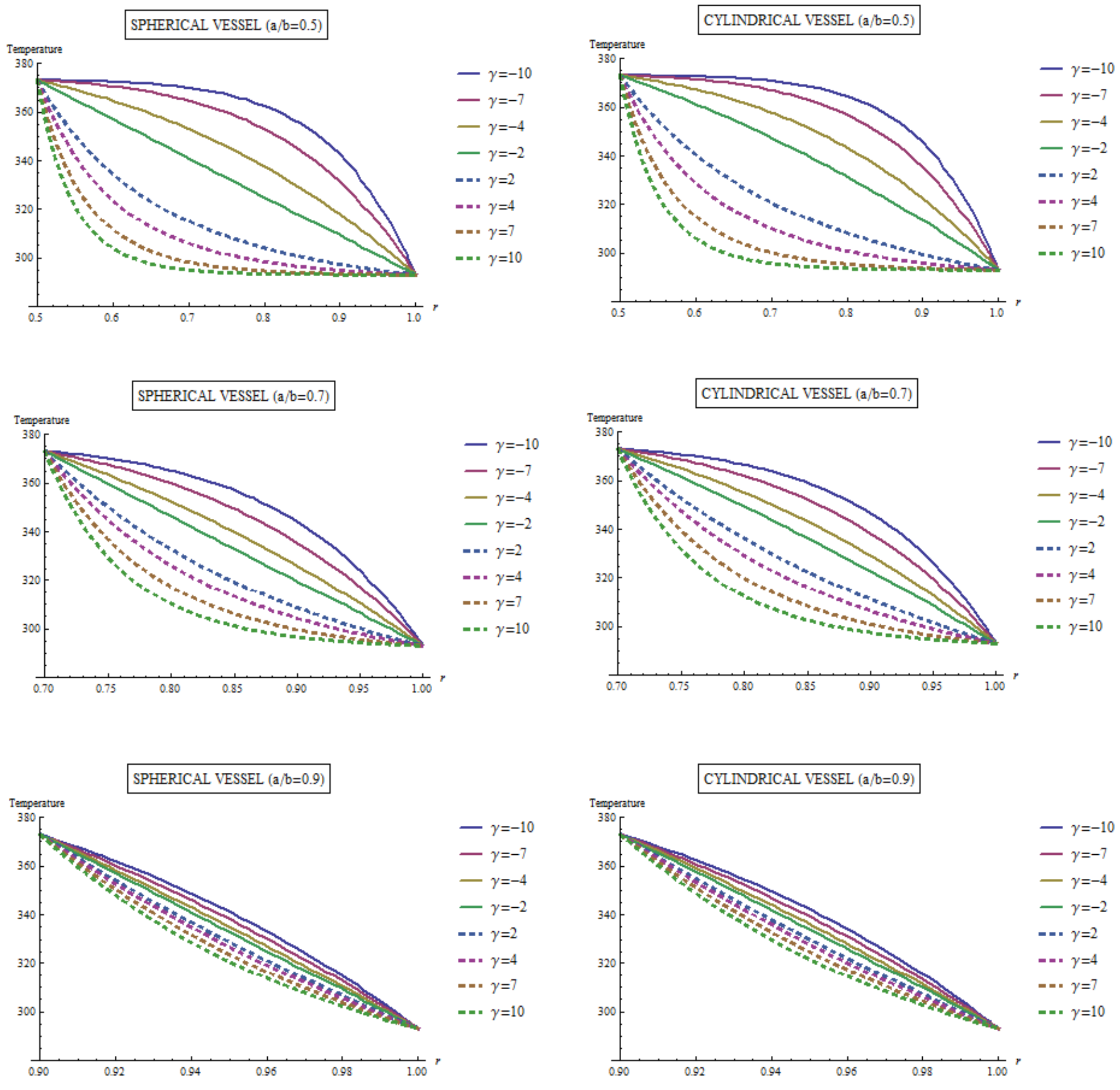

Fig. 4. Variation of temperature with hypothetic inhomogeneity indexes and aspect ratios for both cylinders and spheres ($k_a = 20$ W/mK)

4. A Parametric Study with Hypothetic Inhomogeneity Indexes

In this section, a parametric study is carried out to investigate the temperature variation along the radial direction with both aspect ratios and hypothetic inhomogeneity indexes which vary from $\gamma = -10$ towards $\gamma = 10$. Results are given in Table 4 and Figs. 4 and 5.

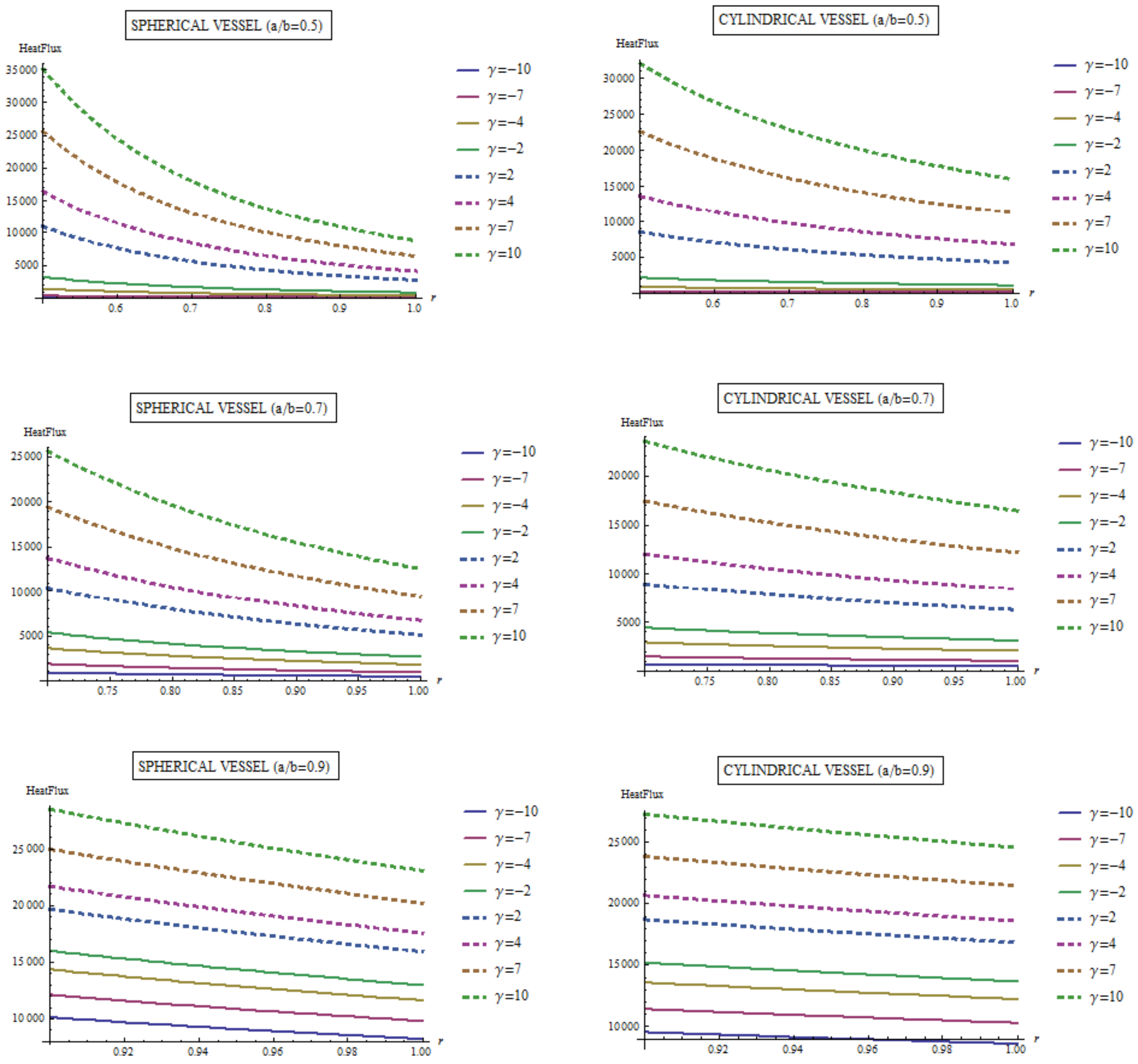

Fig. 5. Variation of heat flux with hypothetic inhomogeneity indexes and aspect ratios for both cylinders and spheres ($k_a = 20$ W/mK)

Table 3. Radial variation of temperature and heat flux with hypothetic inhomogeneity indexes for both cylinders and spheres having $\frac{a}{b}=0.5$ and $k_a = 20$ W/mK.

	$\gamma=-10$	$\gamma=-7$	$\gamma=-4$	$\gamma=-2$	$\gamma=2$	$\gamma=4$	$\gamma=7$	$\gamma=10$
				$T_{sphere}(r)$				
0.5	373.	373.	373.	373.	373.	373.	373.	373.
0.55	372.787	372.02	369.217	365.	350.263	341.695	330.153	321.014
0.6	372.349	370.478	364.68	357.	334.481	323.607	311.365	303.733
0.65	371.496	368.141	359.32	349.	323.187	312.661	302.532	297.427
0.7	369.922	364.709	353.069	341.	314.891	305.774	298.128	294.937
0.75	367.138	359.806	345.857	333.	308.661	301.294	295.82	293.886
0.8	362.398	352.965	337.617	325.	303.893	298.295	294.556	293.416
0.85	354.591	343.619	328.28	317.	300.181	296.235	293.838	293.194
0.9	342.102	331.08	317.777	309.	297.248	294.79	293.415	293.085
0.95	322.638	314.529	306.04	301.	294.901	293.754	293.159	293.03
1.	293.	293.	293.	293.	293.	293.	293.	293.
				$T_{cylinder}(r)$				
0.55	372.875	372.402	370.525	367.4	354.488	345.95	333.746	323.795
0.6	372.594	371.373	367.274	361.267	340.407	328.819	314.872	305.855
0.65	372.	369.677	363.101	354.6	329.45	317.544	305.22	298.731
0.7	370.816	366.99	357.845	347.4	320.755	309.88	300.019	295.69
0.75	368.569	362.867	351.333	339.667	313.741	304.523	297.089	294.31
0.8	364.48	356.721	343.381	331.4	308.	300.688	295.374	293.65
0.85	357.313	347.782	333.789	322.6	303.242	297.884	294.335	293.319
0.9	345.157	335.065	322.346	313.267	299.255	295.796	293.687	293.146
0.95	325.132	317.323	308.829	303.4	295.881	294.215	293.272	293.052
				$q_{r-sphere}(r)$				
0.5	56.3601	304.762	1371.43	3200.	10971.4	16516.1	25700.4	35217.2
0.55	46.5786	251.869	1133.41	2644.63	9067.3	13649.7	21240.	29105.1
0.6	39.1389	211.64	952.381	2222.22	7619.05	11469.5	17847.5	24456.4
0.65	33.3492	180.332	811.496	1893.49	6491.97	9772.86	15207.3	20838.6
0.7	28.7551	155.491	699.708	1632.65	5597.67	8426.6	13112.4	17968.
0.75	25.0489	135.45	609.524	1422.22	4876.19	7340.5	11422.4	15652.1
0.8	22.0157	119.048	535.714	1250.	4285.71	6451.61	10039.2	13756.7
0.85	19.5018	105.454	474.543	1107.27	3796.34	5714.92	8892.87	12185.9
0.9	17.3951	94.0623	423.28	987.654	3386.24	5097.57	7932.22	10869.5
0.95	15.6122	84.4216	379.897	886.427	3039.18	4575.1	7119.22	9755.46
1.	14.09	76.1905	342.857	800.	2742.86	4129.03	6425.1	8804.3
				$q_{r-cylinder}(r)$				
0.5	31.2805	176.378	853.333	2133.33	8533.33	13653.3	22576.4	32031.3
0.55	28.4369	160.344	775.758	1939.39	7757.58	12412.1	20524.	29119.3
0.6	26.0671	146.982	711.111	1777.78	7111.11	11377.8	18813.6	26692.7
0.65	24.062	135.675	656.41	1641.03	6564.1	10502.6	17366.4	24639.4
0.7	22.3432	125.984	609.524	1523.81	6095.24	9752.38	16126.	22879.5
0.75	20.8537	117.585	568.889	1422.22	5688.89	9102.22	15050.9	21354.2
0.8	19.5503	110.236	533.333	1333.33	5333.33	8533.33	14110.2	20019.6
0.85	18.4003	103.752	501.961	1254.9	5019.61	8031.37	13280.2	18841.9
0.9	17.3781	97.9878	474.074	1185.19	4740.74	7585.19	12542.4	17795.2
0.95	16.4634	92.8305	449.123	1122.81	4491.23	7185.96	11882.3	16858.6
1.	15.6403	88.189	426.667	1066.67	4266.67	6826.67	11288.2	16015.6

As seen from Table 3, metals have much greater thermal conductivities than ceramics. If Eq. (10) is considered, that is if a metal is placed on the inner surface, this produces negative inhomogeneity indexes. The converse is true if a ceramic is on the inner surface. When the inhomogeneity index is changed from $\gamma = -10$ to $\gamma = 10$, the temperature declines faster at the vicinity of the inner surface (Fig. 4). Maximum heat flux is at the inner surface for all conditions since the inner surface has greater temperature than the outer. Heat flux decreases with negative inhomogeneity indexes (Fig. 5).

5. Conclusions

This study offers compact expressions in closed forms for the temperature and the heat-flux distributions in radial direction for hollow cylindrical and spherical structures made of radially functionally graded materials. A simple power material grading rule is used to get a differential equation with constant coefficients.

The derived formula for the temperature distribution becomes indefinite at $\gamma = -1$ in spheres and $\gamma = 0$ in cylinders. This disadvantage may be overcome numerically by using real numbers instead integers for those inhomogeneity indexes as seen in Fig. 2.

The formulas in Tables 1 and 2 may be used directly in some thermal and optimization problems. They may also be served as sound benchmark results for advanced studies.

Notations

a	radius at the inner surface
b	radius at the outer surface
c_p	specific heat capacity $\left(J/(kgK)\right)$
C_1, C_2	integration constants
$\boldsymbol{e_r}, \boldsymbol{e_\theta}, \boldsymbol{e_z}$	unit vectors in cylindrical coordinates
$\boldsymbol{e_r}, \boldsymbol{e_\theta}, \boldsymbol{e_\varphi}$	unit vectors in spherical coordinates
k	thermal conductivity $\left(W/(mK)\right)$
q or q_r	Heat flux component in radial direction
$\boldsymbol{q}$	the rate of heat flux vector (W/m^2)
$\dot{q}_{gen}$	heat generation per unit volume
r	radial coordinate
t	time
T	temperature
γ	inhomogeneity constant for simple-power grading rule
$\kappa = \frac{\rho c_p}{k}$	thermal diffusion coefficient (m^2/s)
μ_1, μ_2	characteristic roots of the differential equation
ρ	density (kg/m^3)
θ	Azimuthal angle
φ	Zenith angle
∇	gradient operator

$\nabla^2 = \Delta$	Laplacian operator
$\frac{d}{dr}(\,) = (\,)'$	derivative with respect to the radial coordinate
subscripts	
a	value at the inner surface
b	value at the outer surface

References

[1] Chang, Y.P., Tsou, R.C.H., Heat conduction in an anisotropic medium homogeneous in cylindrical regions—steady state. *ASME J. Heat Transfer*, 99(1), 132–134. 1977.

[2] Chang, Y. P., Tsou, R.C.H., Heat conduction in an anisotropic medium homogeneous in cylindrical coordinates-unsteady state. *ASME J. Heat Transfer*, 99(1), 41–46, 1977.

[3] Ootao, Y., Tanigawa, Y., Fukuda T., Axisymmetric transient thermal stress analysis of a multilayered composite hollow cylinder. *J. Therm. Stresses*, 14(2), 201-213, 1991.

[4] Obata, Y., Noda, N., Steady thermal stresses in a hollow circular cylinder and a hollow sphere of a functionally gradient material. *J. Therm. Stresses*, 17(3), 471–487, 1994.

[5] Zimmerman, R.W., Lutz, M.P., Thermal stresses and thermal expansion in a uniformly heated functionally graded cylinder. *J. Therm. Stresses*, 22 (2), 177–188, 1999.

[6] Tarn, J.Q., Exact solutions for functionally graded anisotropic cylinders subjected to thermal and mechanical loads. *Int. J. Solids Struct*., 38, 8189–8206, 2001.

[7] Awaji, H., Sivakuman, R., Temperature and stress distributions in a hollow cylinder of functionally graded material: the case of temperature-dependent material properties. *Journal of American Ceramic Society*, 1059-1065, 2001.

[8] Jabbari, M., Sohrabpor, S., Eslami, M.R., Mechanical and thermal stresses in a functionally graded hollow cylinder due to radially symmetric loads. *Int. J. Pressure Vessels Piping*, 79, 493–497, 2002.

[9] Jabbari, M., Sohrabpour, S., Eslami, M.R., General solution for mechanical and thermal stresses in a functionally graded hollow cylinder due to nonaxisymmetric steady-state loads. *ASME J. Appl. Mech*., 70 , 111–118, 2003.

[10] Jabbari, M., Bahtui, A., Eslami, M.R., Axisymmetric mechanical and thermal stresses in thick long FGM cylinders. *J. Therm. Stresses*, 29 (7), 643–663, 2006.

[11] Liew, K.M., Kitipornchai, S., Zhang, X.Z., Lim, C.W., Analysis of the thermal stress behaviour of functionally graded hollow circular cylinders. *Int. J. Solids Struct*., 40, 2355–2380, 2003.

[12] Tarn, J.Q., Wang, Y.M., End effects of heat conduction in circular cylinders of functionally graded materials and laminated composites. *Int. J. Heat Mass Transfer*, 47, 5741–5747, 2004.

[13] Ruhi, M., Angoshtari, A., Naghdabadi, R., Thermoelastic analysis of thick-walled finite-length cylinders of functionally graded materials. *J. Therm. Stresses*, 28 (4), 391-408, 2005.

[14] Oral, A., Anlas, G., Effects of radially varying moduli on stress distribution of nonhomogeneous anisotropic cylindrical bodies. *International Journal of Solids and Structures*, 5568–5588, 2005.

[15] Eslami, M.R., Babai, M.H., Poultangari, R., Thermal and mechanical stresses in a functionally graded thick sphere. *Int. J. Pressure Vessels Piping*, 82 (7), 522–527, 2005.

[16] Ootao, Y., Tanigawa, Y., Transient thermoelastic analysis for a functionally graded hollow cylinder. *J. Therm. Stresses*, 29(11), 1031–1046, 2006.

[17] Pelletier, J.L., Vel, S.S., An exact solution for the steady-state thermoelastic response of functionally graded orthotropic cylindrical shells. *Int. J. Solids Struct.*, 43, 1131–1158, 2006.

[18] Birman, V., Byrd., L.W., Modeling and analysis of functionally graded materials and structures. *Applied Mechanics Reviews*, 60, 195-216, 2007.

[19] Kayhani, M.H., Shariati, M., Nourozi, M., Demneh, M.K., Exact solution of conductive heat transfer in cylindrical composite laminate. *Heat Mass Transfer*, 46, 83–94, 2009.

[20] Kayhani, M.H., Norouzi, M., Delouei, A.A., A general analytical solution for heat conduction in cylindrical multilayer composite laminates. *Int. J. Therm. Sci*., 52, 73–82, 2012.

[21] Hosseini, S.M., Abolbashari, M.H., A unified formulation for the analysis of temperature field in a thick hollow cylinder made of functionally graded materials with various grading patterns. *Heat Transfer Eng*., 33, 261–271, 2012.

[22] Bayat, Y., Ghannad, M., Torabi, H., Analytical and numerical analysis for the FGM thick sphere under combined pressure and temperature loading. *Archive of Applied Mechanics*, 229-242, 2012.

[23] Lee, S.Y., Huang, C.C., Analytic solutions for heat conduction in functionally graded circular hollow cylinders with time-dependent boundary conditions. *Mathematical Problems in Engineering*, Article ID 816385, 1-8. 2013.

[24] Wang, H.M., An effective approach for transient thermal analysis in a functionally graded hollow cylinder. *International Journal of Heat and Mass Transfer*, 67, 499-505, 2013.

[25] Li, H., Liu, Y., Functionally graded hollow cylinders with arbitrary varying material properties under non-axisymmetric loads. *Mechanics Research Communications*, 55, 1-9, 2014.

[26] Delouei, A.A., Norouzi, M., Exact analytical solution for unsteady heat conduction in fiber-reinforced spherical composites under the general boundary conditions. *Journal of Heat Transfer*, 137, 1-8. 2015.

[27] Arefi, M., Nonlinear thermal analysis of a hollow functionally graded cylinder with temperature-variable material properties. *Journal of Applied Mechanics and Technical Physics*, 56(2), 267-273, 2015.

[28] Chen, A., Jian, S., Lumped models for transient thermal analysis of multilayered composite pipeline with active heating. *Applied Thermal Engineering*, 87, 749–759, 2015.

[29] Daneshjou, K., Bakhtiari, M., Parsania H., Fakoor, M., Non-Fourier heat conduction analysis of infinite 2D orthotropic FG hollow cylinders subjected to time-dependent heat source. *Applied Thermal Engineering*, 98, 582–590, 2016.

[30] Hetnarski, B., Eslami, M.R., Thermal Stresses-Advanced Theory and Applications, Springer. Chap. 4-ISBN: 978-1-4020-9246-62009.